

The gluonic excitation of the three-quark system in SU(3) lattice QCD

Toru T. Takahashi ^{*}and Hideo Suganuma [†]

November 13, 2018

Abstract

We present the first study of the gluonic excitation in the three-quark (3Q) system in SU(3) lattice QCD with $\beta=5.8$ and $16^3 \times 32$ at the quenched level. For the spatially-fixed 3Q system, we measure the gluonic excited-state potential, which corresponds to the flux-tube vibrational energy in the flux-tube picture. The lowest gluonic-excitation energy in the 3Q system is found to be about 1GeV in the hadronic scale. This large gluonic-excitation energy is expected to bring about the success of the simple quark model without gluonic modes.

The low-lying hadrons are well categorized with the simple quark model, which has only quark degrees of freedom. The success of the quark model implies the absence of the gluonic excitation in the low-lying hadron spectra, which seems rather mysterious. To understand the success of the quark model based on QCD, it is important to investigate the gluonic excitation mode.

Theoretically, the gluonic excitation is expected to appear as the vibrational mode of the squeezed color-flux-tube, which is formed due to color confinement [1, 2]. Experimentally, this type of the gluonic excitation is closely related to the hybrid mesons or the hybrid baryons, which consist of $q\bar{q}G$ or $qqqG$, respectively, in the valence picture. In particular, the several states with the exotic quantum number such as $J^{PC} = 0^{-}, 0^{+-}, 1^{-+}, 2^{+-}, \dots$ cannot be constructed with the simple quark picture[3], and therefore they are now investigated with much attention from both theoretical and experimental viewpoints [4].

For the Q- \bar{Q} system corresponding to mesons, there are several lattice QCD studies for both the ground-state and the excited-state potentials. The lattice QCD study indicates that the Q- \bar{Q} ground-state potential takes the form of $V_{Q\bar{Q}}^{\text{g.s.}}(r) = -A\frac{1}{r} + \sigma r$, as the function of the inter-quark distance r , with $A \simeq 0.27$ and $\sigma \simeq 0.89\text{GeV/fm}$ besides a irrelevant constant [5, 6]. On the other hand, the lowest excited-state potential for the spatially-fixed Q- \bar{Q} system can be fitted as $V_{Q\bar{Q}}^{\text{e.s.}}(r) = \sqrt{b_0 + b_1 r + b_2 r^2} + c_0$ [7]. Here, the quantum number of the first-excited state is $L = 1$ for the magnitude of the projection of the total angular

^{*}Research Center for Nuclear Physics, Osaka University, Mihogaoka 10-1, Ibaraki 567-0047, Japan

[†]Faculty of Science, Tokyo Institute of Technology, Ohokayama 2-12-1, Tokyo 152-8551, Japan

momentum of the gluon onto the $Q\bar{Q}$ axis [7]. The excitation energy $V_{Q\bar{Q}}^{\text{e.s.}} - V_{Q\bar{Q}}^{\text{g.s.}}$ is in the order of 1GeV in the typical hadronic scale as 0.5–1.0fm, and seems rather large in comparison with the low-lying excitation energy of the quark origin.

For the 3Q system corresponding to baryons, the situation is much more complicated. Even for the 3Q ground-state potential, the accurate measurement of the 3Q potential using lattice QCD is relatively difficult and has been performed recently. The recent detailed lattice-QCD analysis indicates the Y-type flux-tube formation in the ground-state 3Q system [5, 6, 8]. The vibrational modes of the Y-type flux tube system are considered to be much more complicated and chaotic than those of the simple $Q\bar{Q}$ flux-tube, owing to the possible interference among the vibrational modes on the three-flux tubes connected at the physical junction, which is not spatially fixed.

Note here that the magnitude of the excitation energy is closely related to the nature of the physical junction. For instance, if the physical junction behaves as a quasi-fixed edge of the three flux tubes, the vibrational energy in the 3Q system would be expressed as a simple sum of the three modes on the $Q\bar{Q}$ system, where the quark and antiquark behave as fixed edges. If the physical junction behaves as a quasi-free edge of the flux tube, the vibrational energy in the 3Q system would be smaller than that in the $Q\bar{Q}$ system with the similar size. (In general in the quantum physics, the vibrational modes on the string with the fixed edges becomes large.)

To begin with, we briefly review the lattice-QCD measurement of the 3Q ground-state potential from the 3Q Wilson loop using the smearing method [5, 6]. Similar to the $Q\bar{Q}$

Figure 1: The 3Q Wilson loop W_{3Q} . The gauge-invariant 3Q state is generated at $t = 0$ and is annihilated at $t = T$. The three quarks are spatially fixed in \mathbf{R}^3 for $0 < t < T$.

potential measured with the Wilson loop, the 3Q potential can be measured with the 3Q Wilson loop W_{3Q} defined as

$$W_{3Q} \equiv \frac{1}{3!} \varepsilon_{abc} \varepsilon_{a'b'c'} U_1^{aa'} U_2^{bb'} U_3^{cc'} \quad (1)$$

with $U_k \equiv \text{P exp}\{ig \int_{\Gamma_k} dx^\mu A_\mu(x)\}$ ($k = 1, 2, 3$). Here, P denotes the path-ordered product along the path denoted by Γ_k in Fig. 1. The ground-state potential $V_{3Q}^{\text{g.s.}}$ can be obtained from the expectation value $\langle W_{3Q}(T) \rangle$ of the 3Q Wilson loop in the large limit of its temporal length T as $V_{3Q}^{\text{g.s.}} = -\lim_{T \rightarrow 0} \frac{1}{T} \ln \langle W_{3Q}(T) \rangle$. In the practical lattice calculation, one has

to take enough large T where the excited-state contributions drop, but $\langle W_{3Q}(T) \rangle$ itself exponentially decreases with T , which makes the accurate measurement difficult.

Then, for the accurate measurement, we apply the smearing method, a useful standard technique to enhance the ground-state component in the 3Q operator W_{3Q} [5, 6]. The smearing is defined as the iterative replacement of the spatial link variables by the “fat” link variables, and refines the 3Q operator to have a large overlap with the ground state of the 3Q system. In fact, spatial link variables $U_i(s)$ are replaced by the new link variables $\bar{U}_i(s)$ defined so as to maximize

$$\text{Re tr} \left\{ \bar{U}_i^\dagger(s) \left[\alpha U_i(s) + \sum_{j \neq i} \{ U_j(s) U_i(s + \hat{j}) U_j^\dagger(s + \hat{i}) + U_j^\dagger(s - \hat{j}) U_i(s - \hat{j}) U_j(s + \hat{i} - \hat{j}) \} \right] \right\}, \quad (2)$$

where we adopt $\alpha = 2.3$ for the smearing parameter. This replacement is iterated until the overlap of the 3Q operator with the ground state is maximized, i.e., the contamination of the excited states is minimized. For instance, as the iteration number N_{smr} of the smearing increases from $N_{\text{smr}}=0$, the excited-state components in the N_{smr} -th smeared operator gradually decrease, and finally the 22th smeared operator is almost ground-state saturated for $\alpha = 2.3$ on the lattice with $\beta = 5.8$ [6].

Using the suitable smeared link-variable, we reconstruct the generalized 3Q Wilson loop $\langle W_{3Q}(T) \rangle$. Then, one finds $V_{3Q}^{\text{g.s.}} \simeq -\frac{1}{T} \ln \langle W_{3Q}(T) \rangle$ even at small T , and one can perform the accurate measurement of $V_{3Q}^{\text{g.s.}}$. From the recent detailed analysis of the static 3Q potential in Refs. [5, 6], the ground-state 3Q potential $V_{3Q}^{\text{g.s.}}$ is found to be expressed as

$$V_{3Q}^{\text{g.s.}} = -A_{3Q} \sum_{i < j} \frac{1}{|\mathbf{r}_i - \mathbf{r}_j|} + \sigma_{3Q} L_{\text{min}} + C_{3Q}, \quad (3)$$

where L_{min} denotes the minimal value of the total length of color-flux-tubes linking the three quarks [1, 2, 9]. (The observation of the Y-type flux-tube profile is also reported in lattice QCD [8].)

Next, we present the formalism to extract the excited-state potential. For the simple notation, the ground state is regarded as the “0-th excited state” in this paper. For the physical eigenstates of the QCD Hamiltonian \hat{H} for the spatially-fixed 3Q system, we denote the n -th excited state by $|n\rangle$ ($n=0,1,2,3,\dots$). Since the three quarks are spatially fixed in this case, the eigenvalue of \hat{H} is expressed by the static 3Q potential as

$$\hat{H}|n\rangle = E_n|n\rangle = V_n|n\rangle, \quad (4)$$

where V_n denotes the n -th excited-state 3Q potential. We take the normalization condition as $\langle m|n\rangle = \delta_{mn}$. Note that both V_n and $|n\rangle$ ($n = 0, 1, 2, \dots$) are universal physical quantities relating to the QCD Hamiltonian \hat{H} .

Suppose that $|\Phi_k\rangle$ ($k = 0, 1, 2, 3, \dots$) are arbitrary given independent 3Q operators for the spatially-fixed 3Q system. In general, each 3Q operator $|\Phi_k\rangle$ can be expressed with a linear combination of the physical eigenstates $|n\rangle$ ($n = 0, 1, 2, \dots$) as

$$|\Phi_k\rangle = c_0^k|0\rangle + c_1^k|1\rangle + c_2^k|2\rangle + \dots \quad (5)$$

Here, the coefficients c_n^k depend on the selection of the 3Q operators $|\Phi_k\rangle$, and hence they are not universal quantities. (Unlike the Q- \bar{Q} system, there is no definite symmetry in the 3Q system, and hence we do not construct the operators which carry the specific quantum number.)

The Euclidean time-evolution of the 3Q state $|\Phi(t)\rangle$ is expressed with the operator $e^{-\hat{H}t}$, which corresponds to the transfer matrix in lattice QCD. The overlap $\langle\Phi_j(T)|\Phi_k(0)\rangle$ is given by the 3Q Wilson loop sandwiched by the initial state Φ_k at $t = 0$ and the final state Φ_j at $t = T$, and is expressed in the Euclidean Heisenberg picture as

$$\begin{aligned} W_T^{jk} &\equiv \langle\Phi_j(T)|\Phi_k(0)\rangle = \langle\Phi_j|W_{3Q}(T)|\Phi_k\rangle = \langle\Phi_j|e^{-\hat{H}T}|\Phi_k\rangle \\ &= \sum_{m=0}^{\infty} \sum_{n=0}^{\infty} \bar{c}_m^j c_n^k \langle m|e^{-\hat{H}T}|n\rangle = \sum_{n=0}^{\infty} \bar{c}_n^j c_n^k e^{-V_n T}. \end{aligned} \quad (6)$$

We define the matrix C and the diagonal matrix Λ_T by $C^{nk} = c_n^k$, $\Lambda_T^{mn} = e^{-V_n T} \delta^{mn}$, and rewrite the above relation as

$$W_T = C^\dagger \Lambda_T C. \quad (7)$$

Note here that C is not a unitary matrix, and hence this relation does not mean the simple diagonalization by the unitary transformation, which connects the two matrices by the similarity transformation.

Since we are interested in the 3Q potential V_n ($n = 0, 1, 2, \dots$) in Λ_T rather than the non-universal matrix C , we single out V_n from the 3Q Wilson loop W_T using the following prescription. From Eq.(7), we obtain

$$\begin{aligned} W_T^{-1} W_{T+1} &= \{C^\dagger \Lambda_T C\}^{-1} C^\dagger \Lambda_{T+1} C \\ &= C^{-1} \Lambda_T^{-1} \Lambda_{T+1} C \\ &= C^{-1} \text{diag}(e^{-V_0}, e^{-V_1}, \dots) C. \end{aligned} \quad (8)$$

Now the r.h.s is expressed by the l.h.s with the similarity transformation. Therefore, e^{-V_n} can be obtained as the eigenvalues of the matrix $W_T^{-1} W_{T+1}$, i.e., the solutions of the secular equation,

$$\begin{aligned} \det\{W_T^{-1} W_{T+1} - tI\} &= \det\{\Lambda_T^{-1} \Lambda_{T+1} - tI\} \\ &= \prod_n (e^{-V_n} - t) = 0, \end{aligned} \quad (9)$$

where I denotes the unit matrix. The largest eigenvalue corresponds to e^{-V_0} and the n -th largest eigenvalue corresponds to e^{-V_n} .

In this way, the 3Q potential V_n ($n = 0, 1, 2, \dots$) can be obtained from the matrix $W_T^{-1} W_{T+1}$. In the practical calculation, we prepare N independent sample operators $|\Phi_k\rangle$ ($k = 0, 1, \dots, N-1$). If one chooses appropriate operators $|\Phi_k\rangle$ so as not to include highly excited-state components, one can truncate the physical states as $|n\rangle$ ($n = 0, 1, 2, \dots, N-1$). Then, W_T , C and Λ_T are reduced into $N \times N$ matrices, and the secular equation Eq.(9) becomes the N -th order equation.

Now, we study the ground-state potential $V_{3Q}^{\text{g.s.}}$ and the 1st excited-state potential $V_{3Q}^{\text{e.s.}}$ for the spatially-fixed 3Q system in SU(3) lattice QCD with $\beta=5.8$ and $16^3 \times 32$ at the quenched level. The lattice spacing is found to be $a \simeq 0.14\text{fm}$, which reproduces the string tension $\sigma=0.89\text{GeV/fm}$ in the Q- \bar{Q} potential.

In this paper, we concentrate ourselves on the ground state $|0\rangle$ and the 1st excited state $|1\rangle$ in the spatially-fixed 3Q system. To extract V_0 and V_1 , we need to prepare at least two independent operators $|\Phi_k\rangle (k = 0, 1)$, and construct the 2×2 matrix $W_T^{-1}W_{T+1}$ with them. Here, the sample operators $|\Phi_k\rangle$ can be freely chosen, as long as they satisfy the two conditions: the linear independence and the smallness of the higher excited-state components $|n\rangle$ with $n \geq 2$, which leads to $|\Phi_k\rangle \simeq c_0^k|0\rangle + c_1^k|1\rangle$.

As the sample 3Q operators $|\Phi_k\rangle$, we adopt the properly smeared 3Q operators since the higher excited-state components are reduced in them [6]. After some numerical check on the above two conditions, we adopt the 8th, 12th, 16th, 20th smeared 3Q operators as the candidates of the sample 3Q operators. (Owing to the intervals of 4 iterations, these smeared operators are clearly independent each other. The N_{smr} -th smeared operator with $N_{\text{smr}} \geq 8$ has small higher excited-state components.)

Figure 2: An example of the effective-mass plot for $V_0(T)$ (open circles) and $V_1(T)$ (filled circles) obtained from the eigenvalues of $W_T^{-1}W_{T+1}$ at each T for the spatially-fixed three quarks put on $(1, 0, 0)$, $(0, 1, 0)$ and $(0, 0, 1)$ in the lattice unit. For both $V_0(T)$ and $V_1(T)$ at each T , we plot 6 data obtained from the 6 pairs of the operator combination.

For each pair of these 4 operators, we calculate the generalized 3Q Wilson loop $W_T^{jk} \equiv \langle \Phi_j(T) | \Phi_k(0) \rangle$, and evaluate V_0 and V_1 using Eq.(9). We plot in Fig. 2 an example of the “effective mass” plot for $V_0(T)$ and $V_1(T)$ obtained from Eq.(9) at each T as the function of the temporal separation T . On the statistical error of the lattice data, we adopt the jackknife error estimate.

For both $V_0(T)$ and $V_1(T)$ at each T , we obtain the 6 data obtained from the 6 pairs of the operator combination among the 8th, 12th, 16th, 20th smeared 3Q operators. As shown in Fig.2, these 6 data almost coincide and the T -dependence of $V_0(T)$ and $V_1(T)$ is

rather small in a certain region of T . This indicates the smallness of the higher excited-state components $|n\rangle$ with $n \geq 2$ in the sample operators because such contaminations provide a T -dependence in $V_0(T)$ and $V_1(T)$ and make the stability lost.

For the accurate measurement, we select the best pair of two operators providing the most stable effective-mass plot, which physically means the smallest contamination of the higher excited states in them. With the selected two operators, we extract the ground-state potential $V_{3Q}^{\text{g.s.}}$ and the 1st excited-state potential $V_{3Q}^{\text{e.s.}}$ using the χ^2 fit as $V_{3Q}^{\text{g.s.}} = V_0(T)$ and $V_{3Q}^{\text{e.s.}} = V_1(T)$ in the fit range of T , where the plateau is observed. We perform the above procedure for each 3Q system.

In Table 1, we summarize the lattice QCD results for the 3Q potentials, $V_{3Q}^{\text{g.s.}}$ and $V_{3Q}^{\text{e.s.}}$ for the 24 different patterns of the spatially-fixed 3Q system. In Fig. 3, we plot the ground-state potential and the 1st excited-state potential as the function of L_{min} in the physical unit.

We attempt to compare $V_{3Q}^{\text{e.s.}}$ with $V_{Q\bar{Q}}^{\text{e.s.}}$ or its linear combinations, since $V_{3Q}^{\text{e.s.}}$ would exhibit a similarity to $V_{Q\bar{Q}}^{\text{e.s.}}$ if the junction of the Y-type flux tube is a quasi-fixed edge. However, there seems no simple relation between $V_{3Q}^{\text{e.s.}}$ and $V_{Q\bar{Q}}^{\text{e.s.}}$, which would reflect the complicated vibrational mode of the Y-type flux tube. On the contrary, $V_{3Q}^{\text{e.s.}}$ does not increase at the short distance, unlike the lowest gluonic-excitation mode in the Q- \bar{Q} system [7]. Such a difference may indicate the quasi-free behavior of the junction of the Y-type flux tube.

Figure 3: The lattice QCD results of the ground-state 3Q potential $V_{3Q}^{\text{g.s.}}$ (open circles) and the 1st excited-state 3Q potential $V_{3Q}^{\text{e.s.}}$ (filled circles) plotted against L_{min} , the minimal total length of flux-tubes linking the three quarks.

As a remarkable fact, the lowest gluonic-excitation energy is found to be about 1GeV in the hadronic scale as $L_{\text{min}} \simeq 0.5 - 1.5\text{fm}$. This is rather large in comparison with the low-lying excitation energy of the quark origin. Also for the Q- \bar{Q} system, the gluonic-excitation energy seems rather large [7]. Owing to the large gluonic-excitation energy, the gluonic excitation mode is invisible in the low-lying excitations of hadrons, which is a reason of the success of the simple quark model without gluonic modes. Such a gluonic excitation would contribute significantly to the highly-excited baryons with the mass above 2GeV, and the

Table 1: The ground-state 3Q potential $V_{3Q}^{\text{g.s.}}$ and the 1st excited-state 3Q potential $V_{3Q}^{\text{e.s.}}$ in the lattice unit. The label (l, m, n) denotes the 3Q system where the three quarks are put on $(la, 0, 0)$, $(0, ma, 0)$ and $(0, 0, na)$ in \mathbf{R}^3 .

(l, m, n)	$V_{3Q}^{\text{e.s.}}$	$V_{3Q}^{\text{g.s.}}$	$V_{3Q}^{\text{e.s.}} - V_{3Q}^{\text{g.s.}}$
(0,1,1)	1.9816(95)	0.7711(3)	1.2104
(0,1,2)	1.9943(72)	0.9682(4)	1.0261
(0,1,3)	2.0252(92)	1.1134(7)	0.9118
(0,2,2)	2.0980(80)	1.1377(6)	0.9603
(0,2,3)	2.1551(87)	1.2686(9)	0.8866
(0,3,3)	2.2125(114)	1.3914(13)	0.8211
(1,1,1)	2.0488(90)	0.9176(4)	1.1312
(1,1,2)	2.0727(75)	1.0686(5)	1.0041
(1,1,3)	2.1023(73)	1.2004(7)	0.9019
(1,1,4)	2.1580(93)	1.3201(10)	0.8380
(1,2,2)	2.1405(72)	1.1907(7)	0.9498
(1,2,3)	2.1899(71)	1.3084(9)	0.8815
(1,2,4)	2.2516(79)	1.4221(12)	0.8296
(1,3,4)	2.2907(91)	1.5260(15)	0.7647
(1,4,4)	2.3807(138)	1.6322(20)	0.7485
(2,2,2)	2.1776(111)	1.2844(10)	0.8932
(2,2,3)	2.2242(96)	1.3882(11)	0.8360
(2,2,4)	2.2799(98)	1.4952(15)	0.7847
(2,3,4)	2.3637(100)	1.5853(18)	0.7784
(2,4,4)	2.4108(137)	1.6836(23)	0.7271
(3,3,3)	2.3408(168)	1.5680(19)	0.7728
(3,3,4)	2.3958(151)	1.6635(22)	0.7323
(3,4,4)	2.4645(177)	1.7565(30)	0.7081
(4,4,4)	2.5245(340)	1.8408(42)	0.6837

lowest hybrid baryon, which is described as $qqqG$ in the valence picture, is expected to have a large mass of about 2GeV. In any case, the present lattice QCD data would provide the useful input in the potential model calculation for the hybrid baryons.

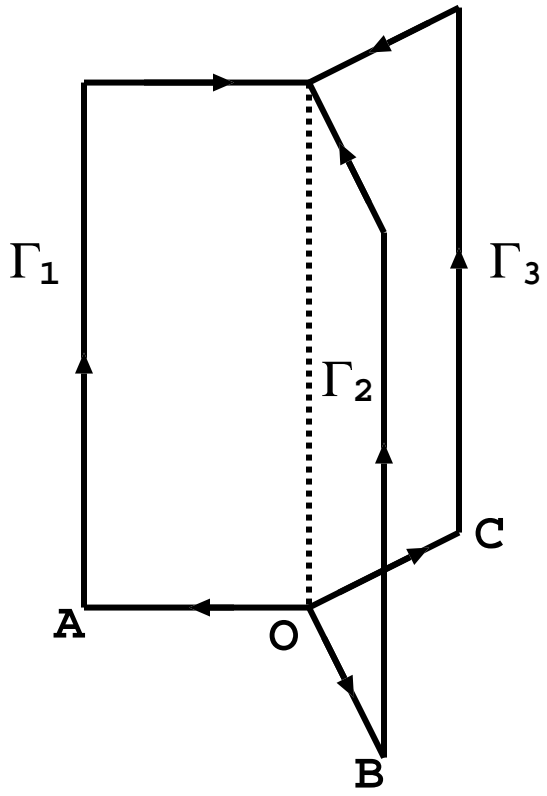
We have studied the gluonic excitation in the three-quark (3Q) system using SU(3) lattice QCD with $\beta=5.8$ and $16^3 \times 32$ at the quenched level. For the 24 different patterns of the spatially-fixed 3Q system, we have measured the gluonic excited-state potential, which corresponds to the flux-tube vibrational energy in the flux-tube picture. As a result, we have found that the lowest gluonic-excitation energy is about 1GeV in the hadronic scale, which is rather large in comparison with the low-lying excitation energy of the quark origin. This large gluonic-excitation energy leads to the absence of the gluonic mode in the low-lying hadrons and brings about the success of the quark model.

One of the author (H.S.) is supported in part by Grant for Scientific Research (No,12640274)

from the Ministry of Education, Culture, Science and Technology, Japan. The lattice QCD calculations have been performed on HITACHI-SR8000 at KEK.

References

- [1] J. Kogut and L. Susskind, Phys. Rev. **D11**, 395 (1975).
- [2] S. Capstick and N. Isgur, Phys. Rev. **D34** 2809, (1986).
- [3] J.F. Donoghue et al., “Dynamics of the Standard Model”, (Cambridge University Press, 1992).
- [4] S. Capstick and P.R. Page, nucl-th/0207027 (2002).
- [5] T.T. Takahashi, H. Matsufuru, Y. Nemoto and H. Suganuma, Phys. Rev. Lett. **86**, 18 (2001).
- [6] T.T. Takahashi, H. Suganuma, Y. Nemoto and H. Matsufuru, Phys. Rev. **D65**, 114509 (2002).
- [7] K.J. Juge, J. Kuti and C.J. Morningstar, Nucl. Phys. **B(Proc.Suppl.)63**, 326 (1998); hep-lat/0207004 (2002).
- [8] H. Ichie, V. Bornyakov, G. Schierholz and T. Streuer, Proc. of Lattice 2002, Nucl. Phys. **B (Proc.Suppl.)**.
- [9] N. Brambilla, G.M. Prosperi and A. Vairo, Phys. Lett. **B362**, 113 (1995).



"Effective Mass" plot

